EPR Studies of the Coverage Effects in TiO$_2$(B)-Supported Vanadia Catalysts for Toluene Ammoxidation

SUSAN JANSEN,[*,1] YANPING TU,[*] MICHAEL J. PALMIERI,[*] MEHRI SANATI,
AND ARNE ANDERSSON[†]

*Department of Chemistry, Temple University, Philadelphia, Pennsylvania 19122; and †Department of
Chemical Technology, Chemical Center, University of Lund, P.O. Box 124, S-221 00 Lund, Sweden*

EPR spectroscopy has been employed to determine the nature of vanadium (+4) species in the TiO$_2$(B)-supported vanadia catalysts. IR and EPR studies show that multiple vanadia species are observed as a function of loading. At coverages greater than 3.5 theoretical layers, the EPR signal is reminiscent of bulk V$_2$O$_5$. At lower coverages, a different magnetic species dominates the resonance and may be attributable to tetrahedral states of vanadium at the oxide interface. The spin concentration and $\langle g \rangle$ suggest two distinct vanadia phases as a function of coverage. In this study, we have also analyzed catalysts after use in ammoxidation of toluene. These samples show strikingly different features compared with the freshly prepared samples. Changes in both the g-anisotropy and hyperfine coupling were observed relative to the fresh catalysts. Though EPR is not surface sensitive, inference into the nature of the catalytic surface can be made by comparison of catalysts of different coverage and studies of monolayer samples. A study of the TiO$_2$(B)–vanadia interface was made by comparing monolayer catalysts prepared from slightly different techniques. Our measurements show strikingly different features in V^{4+} species as a function of preparation. © 1992 Academic Press, Inc.

INTRODUCTION

Titania-supported vanadia is usually used as catalyst for the oxidation and ammoxidation of alkylaromatic compounds to the corresponding anhydrides, acids, aldehydes, and nitriles (1–10). One purpose of using support is to increase the specific area of the active phase, since it is comparatively low for bulk vanadium oxides (11). For the TiO$_2$ support, additionally, an improvement of the catalytic properties, when compared with V$_2$O$_5$, has been observed at low vanadium loadings, which is due to modification of the chemical nature of the surface as a result of active phase–support interaction (7, 12–17).

In industry, usually the anatase polymorph of TiO$_2$ is used as a support for vanadium oxide (18). The improvement of cata-

lytic properties obtained by the use of anatase as support has been explained as due to the formation of highly dispersed vanadia species on the surface. On rutile, the active phase–support interaction is weaker, resulting in formation of crystalline V$_2$O$_5$ (19).

In addition to the vast catalytic data reported on titania supported vanadia catalysts, there is a plethora of studies directed at analysis of the V^{4+} states in the active layers (20–33). In these studies electron paramagnetic resonance (EPR) was utilized to assess the geometry or coordination of the vanadyl and/or V^{4+} species. Though EPR is not surface sensitive, a comparison of the magnetic species as a function of coverage and preparation method allows for a reasonable assessment of surface V^{4+} species. In related studies on supported vanadia catalysts, EPR showed the presence of multiple types of V^{4+} species. The primary spe-

[1] To whom correspondence should be addressed.

cies were V^{4+} in a distorted geometry lying at the interface of the support and active layers, VO^{2+} states, identified by characteristic EPR features, and V^{4+}, from reduced "defect" states in V_2O_5.

Recently, a newly discovered polymorph of TiO_2, called $TiO_2(B)$ (34), has been used as a support for vanadium oxide catalysts (4, 9). Characterization using chemical analysis and diffuse reflectance FTIR (9) showed two types of vanadia distinguishable by their relative solubility in $NH_3(aq)$. Insoluble vanadium was assigned as V^{4+} species interacting with the support. The vanadium not directly bonded to titania is present as V^{5+}. At low loading, both V^{4+} and V^{5+} were concluded to be tetrahedrally coordinated with respect to oxygen. With increase in loading, an abrupt change was observed in which the site symmetry about the vanadium center is now believed due to the formation of octahedral units. At the highest limits, bulk V_2O_5 was observed. Since the structural information derived was the result of infrared spectral features of difference spectra, further study of the system with complementary characterization techniques is of interest.

In this work an EPR study of vanadia supported on $TiO_2(B)$ is presented. Catalytic measurements have shown that this titania phase may provide enhanced activity and selectivity for ammoxidation of toluene (9). However, to date, no EPR study has been reported on the V^{4+} centers on this support.

EXPERIMENTAL

Preparation of the Support

The support material was prepared from TiO_2 (Merck, >99%, 9 m^2/g, anatase) mixed with KNO_3 in a 1.2 : 2 mole ratio. The mixture was calcined at 950°C for 44 hr. X-ray data showed diffraction lines originating from $K_2Ti_4O_9$ only (35). This species was ground and hydrolyzed for three days in excess of 0.45 N HNO_3. After washing, filtration, and drying, the material was calcined in a flow of air at 500°C for 3 hr, yielding a white powder which was shown to be pure $TiO_2(B)$ (36).

Preparation of the Catalysts

The catalysts were prepared by the impregnation technique. A stoichiometric amount of NH_4VO_3 (Merck, p.A.) was added to the desired amount of oxalic acid solution of pH < 1. A deep blue solution was obtained to which the support was added. After evaporation of excess water, the resulting solid material was calcined in a flow of air at 400°C for 3 hr. Sieving provided particles with diameters ranging from 0.150–0.425 mm.

Seven samples with different vanadium loadings were prepared. The loading is included in the catalyst notation in Table 1, e.g., VT-0.3 indicates a loading of V_2O_5/m^2 of support. In Table 1 are also the specific surface areas of support and catalysts, the $V^{4+}/(V^{4+} + V^{5+})$ ratios as they earlier were determined by chemical analysis (9), and the loading expressed in numbers of theoretical V_2O_5 monolayers. The monolayer capacity was determined to correspond to 1.2 mg V_2O_5/m^2 of support (9).

For comparison, a true monolayer sample was prepared by $NH_3(aq)$-treatment of a sample originally having a loading of five theoretical layers. Chemical analysis showed that 80% of the vanadium was dissolved. The remaining layer interacting with the $TiO_2(B)$ surface was present exclusively as V^{4+}.

Catalyst Characterization

X-ray diffraction analysis was carried out using a Philips instrument with a PW 1732/10 generator and Cu$K\alpha$ radiation.

Specific surface areas were determined with a gravimetric BET apparatus using N_2 adsorption at liquid N_2 temperature. The EPR measurements were performed with a Bruker ER-200D system equipped with an ER035 gaussmeter, field frequency controlled and a variable temperature accessory to provide temperature control within 0.5°C.

In addition, to fresh samples, used sam-

TABLE 1

Loading, Surface Area, and Composition of Catalysts

Catalyst	Loading[a] (layers)	S_B[b] (m²/g)	S_A[c] (m²/g)	$V^{+4}/(V^{+4} + V^{+5})$
VT-0.3	0.25	11.0	9.7	0.89
VT-0.6	0.5	15.3	9.8	0.68
VT-0.9	0.75	18.3	13.1	0.52
VT-1.9	1.5	18.3	11.0	0.52
VT-4.2	3.5	13.7	12.7	0.21
VT-6.1	5	13.7	11.4	0.20
VT-12.4	10	13.7	15.7	0.09

[a] No. of theoretical layers assuming 1.2 mg V_2O_5/m² of support for a monolayer.

[b] Surface area/g support before impregnation.

[c] Surface area/g catalyst after impregnation.

ples were prepared for characterization by use in the ammoxidation of toluene. The partial pressures of toluene, NH_3, and oxygen were 0.77, 2.85, and 11.14 kPa, respectively. Catalytic data have been given elsewhere (9).

RESULTS

Chemical Analysis

The results of titrimetric analysis of samples according to the procedures described elsewhere (9) are given in Table 1. At a low loading, the major part of vanadia are present as V^{4+} species. With increase in loading, the amount of V^{5+} increases. For the 5- and 10-layer samples, the fraction of V^{4+} species in relation to the total amount of vanadium is 1/5 and 1/10, respectively. These findings indicate that (i) there is a monolayer of vanadia interacting with the support surface, and (ii) the monolayer species is stabilized in oxidation 4+ in spite of the fact that the samples have been calcined in air at 400°C.

EPR

An analysis of EPR spectra focused on three primary areas of study: (i) Consideration of the coverage effects, characterizing V^{4+} states at submonolayer and multilayer coverages, thus allowing a characterization of the nature of the interface in the low coverage limits; (ii) Comparison of samples after use in ammoxidation reactions with fresh samples; (iii) Analysis of the monolayer or interface states of vanadium at the V_2O_5/TiO₂ interface as a function of preparation. The EPR envelope was not complicated by the support as the TiO₂(B) gave no detectable EPR signal under the conditions of the EPR data collection.

Coverage Dependence of V^{4+} States in Fresh Catalysts

Figure 1 shows the EPR spectral envelope as a function of coverage for several vanadia/TiO₂(B) samples for both room temperature and 100 K. As expected, the low coverage shows spectral features representative of "isolated" vanadium species with the spectral resolution being only slightly enhanced at low temperature. Similar spectra were observed for vanadia supported on other oxide surfaces. For V^{4+} species on anatase or rutile, an axial signal associated with either vanadyl, VO^{2+}, or V^{4+} isolated centers was observed (14, 20, 22, 26). In a few cases, rhombic or orthorhombic symmetry of the g- or A-tensors was noted (14). For the low coverage spectra, the assignment of the components of the g- and A-tensors was made by spectral simulation.
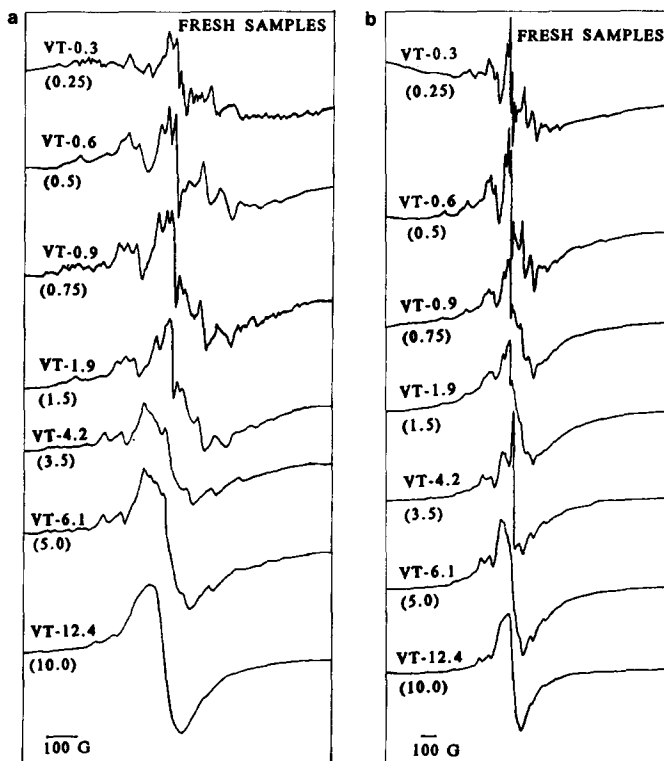
FIG. 1. ESR spectra showing the coverage dependence of vanadia/TiO$_2$(B) for fresh catalysts at room temperature (a) and at 100 K (b). The numbers in parentheses denote the number of theoretical layers.

The program used was developed by Cheyney (37) and is based on application of second order perturbation theory. The primary equations used in this fitting are given below (38–40):

$$H_m(\Theta) = (\omega_0 + KM - (\tfrac{1}{4}\omega_0 K^2))A_\perp^2(A_\parallel^2$$

$$+ K^2)((I + 1) - M^2) - \tfrac{1}{2}\omega_0(A_\parallel^2$$

$$- A_\perp^2/K^2)^2 \sin^2\Theta \cos^2\Theta M^2)/g\beta$$

$$g = (g_\parallel^2 \cos^2\Theta + g_\perp^2 \sin^2\Theta)^{1/2}$$

$$K = (A_\parallel^2 g_\parallel^2 \cos^2\Theta + A_\perp^2 g_\perp^2 \sin^2\Theta)^{1/2}/g.$$

ω_0 is the klystron frequency and $A_\parallel$ and $A_\perp$ are in cm^{-1}.

The results from the fitting suggested the presence of two independent resonances at coverages less than 1.5 monolayers. These were distinguished by differences in both parallel and perpendicular components of the A- and g-tensors. Indication of the components of the hyperfine and g- anisotropy obtained from the simulation is shown in Fig. 2.

In the low coverage samples, 0.25 to 3.5 layers, two magnetic species predominate. From 0.25 to 1 layer the so-called tetrahedral state predominates. In Fig. 2, results of simulation show the primary species at 0.5 layer loading is "tetrahedral," while additional spectral features are noted. These spectral lines appear due to the octahedral component, which increases with increasing loading. This is also indicated in Fig. 2. At higher coverages, e.g., 3.5 layers, the vanadyl octahedral species is dominant. The data from simulation are provided in Fig. 2. No attempt to quantitate the tetrahedral/octahedral concentration was made due to complexity of signal and difficulty in isolation

VT-4.2
3.5-layer "Octahedral"
$A_{//}$ = 198 G $A_\perp$ = 70 G
$g_{//}$ = 1.940 $g_\perp$ = 1.965

3400 G

VT-0.6
1/2-layer "Tetrahedral"
$A_{//}$ = 202 G $A_\perp$ = 79 G
$g_{//}$ = 2.005 $g_\perp$ = 1.980

3350 G   100 G
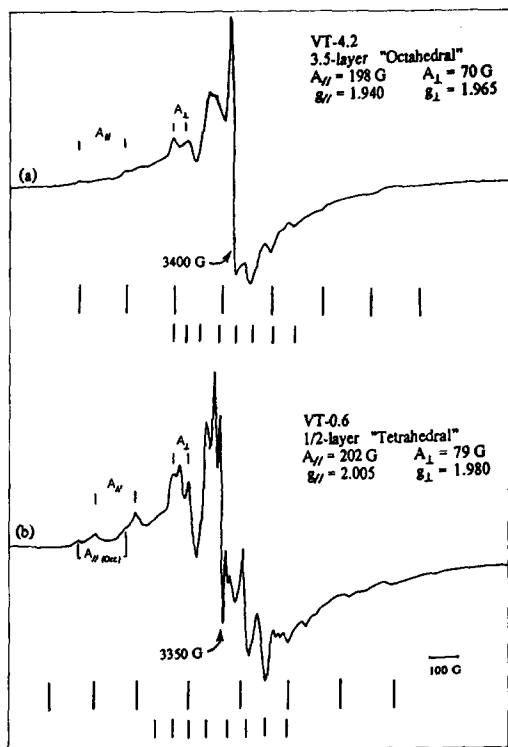
FIG. 2. ESR spectral simulation showing unique V^{4+} states: (a) shows typical vanadyl species as observed at 3.5 layers; (b) shows a predominance of the "tetrahedral" state at low coverage.

of states. Broad spectral features were not included in the simulation as the focus of the investigation was to determine the character of interfacial states predicted by IR studies (9). Simulation of the broad feature is further complicated by the presence of multiple site symmetries persistent even at low loading. It should be stated that the complexity of these spectra precludes a completely unambiguous assignment of the **g**- and **A**-tensor, but analyses based on a single axial or othorhombic species cannot satisfactorily fit these spectra and thus has led to the conclusion that at least two independent magnetic species are present.

A similar observation was made in the case of V^{4+} on anatase. Busca *et al.* (*14*), observed two species characterized by markedly different values of *A*(parallel).

Others have noted the presence of both isolated V^{4+} species exhibiting axial hyperfine and broad line features resulting from dipolar broadening due to V–V interaction (*21, 23, 26, 33*). In each of these cases, the **g**- and **A**-tensors clearly differentiate the unique magnetic species.

As higher loadings are achieved, the spectral envelope shows the effect of increased V–V interaction, with a convergence to V$_2$O$_5$ being observed at 10 theoretical monolayers. The $\langle g \rangle$ as a function of coverage is shown in Fig. 3. This plot suggests that above 3.5 theoretical monolayers, the vanadia character is dominated by a broad line species with a *g*-value similar to that of octahedral or bulk V$_2$O$_5$ like states. The resolution of multiple species and above the five-layer limit, the spectrum obtained appears to originate from a single type of V^{4+} species showing dipolar broadening.

The evaluation of the spin concentration of V^{4+} species shows two critical regions as well. The susceptibility increases in a linear manner up to 1.5 monolayers as is shown in Fig. 4. Above this coverage limit, a second magnetic region is observed. This trend in the spin concentration appears to follow the trend in the *g*'s shown in Fig. 3. In addition, to the two distinct regions of susceptibility, there appears to be a profound coverage induced effect on the spin concentration. At higher coverages, the spin concentrations
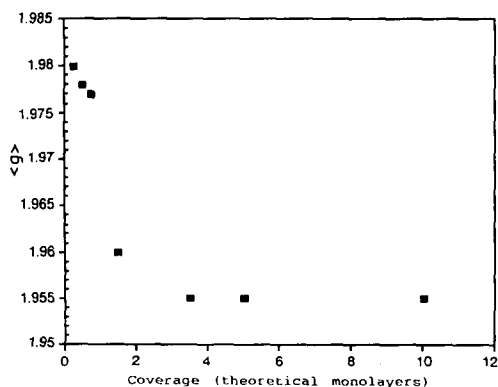
FIG. 3. The $\langle g \rangle$ as a function of coverage.
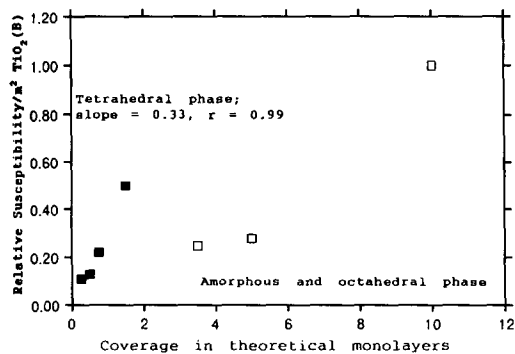
FIG. 4. The evaluation the spin density of V^{4+} species as a function of coverage.

are disproportionately lower than those determined for the coverages less than 1.5 monolayers. A comparison shows that the total spin concentration in the higher coverages is depressed by a factor ranging between 4 and 5. An absolute analysis showed ca. 1.65×10^{-4} mol V^{4+}/g-catalyst for the 1.5-layer catalyst. This value agrees well with the number determined by chemical analysis, 1.82×10^{-4} and is similar in magnitude to the value reported by Dryek et al. (26) for vanadium ions on TiO_2(rutile). The slight depression noted in the measured spin concentration may be due to V^{3+} species present in the vanadia or due to spin coupling.

EPR Spectra of Used Catalysts

Figure 5 shows the catalysts after use in ammoxidation. These spectra show markedly different features compared with the unused catalyst. As in the low coverage cases of the fresh samples, isolated V^{4+} species can be identified with dipolar interactions broadening the spectra above the 3.5-monolayer limit. The assignment of multiple magnetic species in the lower coverages cannot be made absolutely. As a result of the somewhat poorer spectral resolution for these samples, a single set of parallel and perpendicular components of the hyperfine can be resolved. This effect is most apparent in the 0.5-layer sample.

At higher coverages, two spectral features can be easily resolved. In the five-layer sample, a broad line apparently from V_2O_5 like states and a "narrow" species at the center of the resonance window can be observed. These features show different population and saturation phenomena when studied as a function of incident microwave power and thus are easily identified as unique magnetic states. Differential spectral growth rates indicate these signals arise from states with independent relaxation characteristics. A comparison of this five-layer spectrum with those obtained from lower coverages suggests that the narrow species persists even at 0.5 layers and that two unique magnetic species may be present at the lower coverage. Again, the 10-layer sample appears to be a broad line similar to V_2O_5, however, a shoulder is observed at the field position where the narrow line species was observed for the lower coverages. For all coverages, no significant reduction in spin concentration is observed after use in ammoxidation.

Analysis of Vanadia Monolayers on $TiO_2(B)$

In these studies, the EPR results have provided a characterization of states as a function of coverage. A necessary consideration in the development and preparation of useful catalyst concerns the interface properties. In Fig. 1, the 0.75- and 1.5-monolayer samples are representative of the interface preparation by impregnation. For comparison, a true monolayer was prepared by washing the five-layer catalyst with ammonia. The EPR spectra contrasting the theoretical monolayer with the true monolayer produced by the ammonia washing is shown in Fig. 6. Again, striking differences are noted. As previously described, the theoretical monolayer spectrum shows the presence of isolated V^{4+} species, while the spectrum of the true monolayer shows a broad feature in which the hyperfine is not well resolved. The spin concentration is lower in
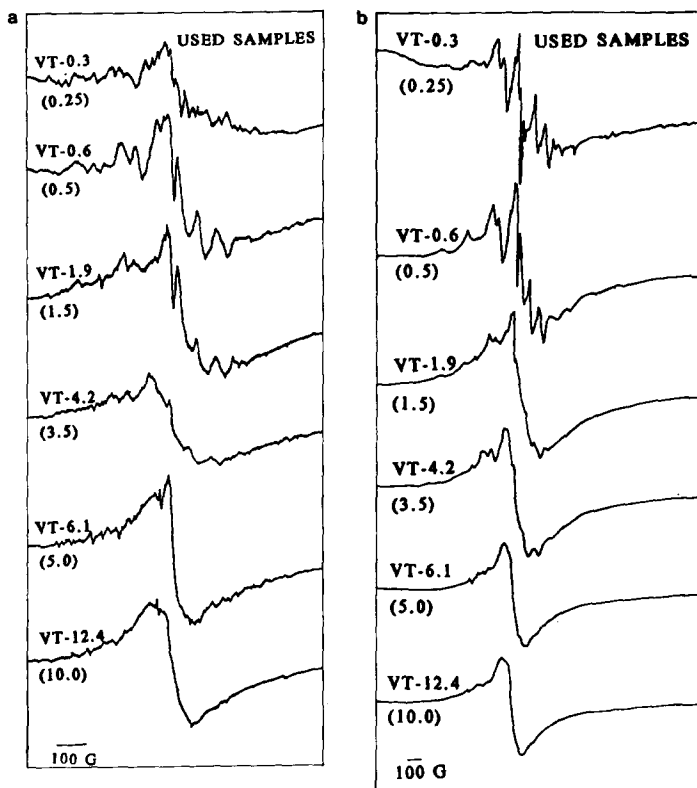
FIG. 5. ESR spectra of coverage dependence of vanadia/TiO$_2$(B) after use in ammoxidation at room temperature (a) and at 100 K (b). The numbers in parentheses denote the number of theoretical layers.

this material as well. The $\langle g \rangle$ value for the true monolayer is ca. 1.96, which is similar the $\langle g \rangle$ value observed for the samples of higher loadings.

DISCUSSION

The results presented here suggest that the interface states are critical in the development of catalysts. In our first study, two types of V^{4+} species were analyzed near and below the theoretical monolayer density; the tetrahedral and well known vanadyl states. In previous analyses of the EPR data on supported vanadia catalysts, Busca et al. (14, 22), Dryek et al. (26), and many others (20, 22) have attributed the axial state with the $g_\perp > g_\parallel$ to VO^{2+} states of the vanadium, possibly in a square pyramidal geometry, as is observed at coverage greater than two monolayers.

The expected $\langle g \rangle$ for pure tetrahedral complexes is predicted to be larger than that of vanadyl species. Tetrahedral states of V^{4+} usually show the g to be on the order of 2.00, with such states being observed for vanadia supported on SiO$_2$ (27), V^{4+} in tetrahedral environments (41). V^{4+} species trapped within a tetrahedral environment in tungstate crystals give $\langle g \rangle$ of 2.002. For tetra-alkyl V^{4+} complexes, the $\langle g \rangle$ ranges from 1.97–1.99 (42–45). The EPR parameters determined at the low coverage; less than two monolayers are similar to those measured for V^{4+} in a tetrahedral field.

Our EPR study shows features and provides observations which are consistent with the vibrational data obtained from these catalysts. FTIR studies on low coverage samples show the presence of tetrahedral V^{4+}, and V^{5+} states, as suggested by
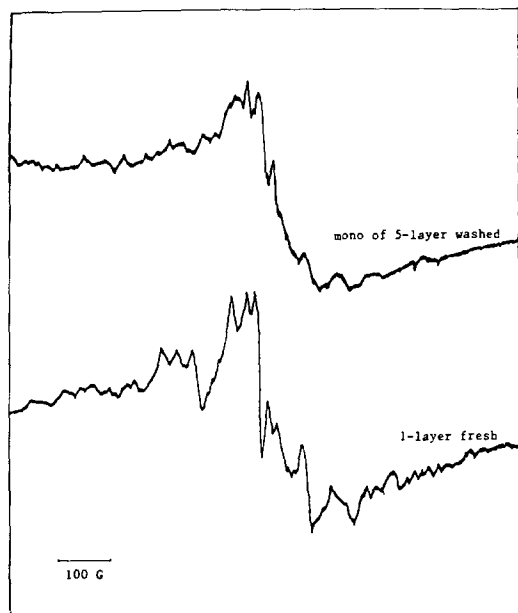
FIG. 6. ESR spectra contrasting the theoretical monolayer with the true monolayer produced by ammonia washing.

this work. As the coverage increases, an octahedral state, the VO^{2+} is formed and at the highest coverage limit, bulk V_2O_5 is observed (9). The spectrum obtained at the highest coverage is dominated by a single broad feature with EPR parameters nearly identical to those of pure V_2O_5.

Our spin concentration measurements on the fresh catalysts show two critical regions as a function of loading, with a distinct divergence at 1.5 monolayers, suggesting a change in the vanadia phase. Chemical analysis of the V^{4+}/V^{5+} content as well as the vibrational spectroscopic results show the same trend. Below two monolayers, the tetrahedral state dominates, then as coverage increases an amorphous state and a V_2O_5 state are identified. From the IR analysis (9), the change in coordination type from tetrahedral to octahedral forms of vanadium was shown to occur near the 3.5-monolayer limit which is the point at which the amorphous phase is first detected. Chemical analysis of the V^{4+}/V_{tot} ratio show that as the

loading is increased the relative amount of V^{4+} in the surface layer decreases, with a dramatic decrease being observed between 1.5 and 3.5 layers. The spin concentration data presented show the total amount of V^{4+} increases, linearly, with loading up to 3.5 monolayers. At this point, the spin concentration or magnetic susceptibility of V^{4+} drops sharply and a new trend is observed up to the highest coverage. The depression in the spin concentration may be due to the formation of a new phase of vanadium in above 3.5 layers, such as the octahedral or bulk V_2O_5 states which are detected by vibrational spectroscopy or to increase the V–V interaction and reduction in the overall spin state. At this critical point, a change in $\langle g \rangle$ is observed also indicative of a change in vanadia character. The absolute values for the spin concentration and V^{4+} concentration obtained from chemical analysis show a different dependence as the EPR measures all V^{4+} species including those dispersed in V_2O_5. The chemical analysis accounts for ammonia soluble and insoluble species based on structure type, with V_2O_5 containing both V^{5+}, the dominant species, and V^{4+}, the minor species, being soluble.

Table 2 shows a correlation of the EPR data with the catalytic and structural properties. The discontinuity in the magnetic susceptibility appears between the tetrahedral and octahedral structural phases though the total spin concentration determined by EPR includes both surface and subsurface vanadia. In comparing these data with the [V(4+)] at the surface, it becomes apparent that the greatest density of reduced vanadium species is at the interface, in a tetrahedral coordination and thus the ratio V^{4+}/V^{5+} is at a relative maximum at low loading. A maximum in catalytic activity and selectivity occurs near the three-layer limit in which there is no significant level of reduced surface vanadia. In this region the structural phase may not be pure. The $\langle g \rangle$ is intermediate between that of the tetrahedral phase and vanadyl species with the IR studies showing both octahedral and V_2O_5 phases

TABLE 2

Surface Composition of Catalysts and Their Performance in the Ammoxidation of Toluene

Catalyst	Surface composition (%)		Rate (μmol m^2 min^{-1})	Selectivity (%)	χ (μmol $-$ V^{4+}/m^2)	$\langle g \rangle$
	TiO$_2$	Vanadia				
VT-0.3	78	19, V^{4+} (tetr) 3, V^{5+} (tetr)	0.33	82	1.81	1.979
VT-0.6	66	9, V^{4+} (tetr) 25, V^{5+} (tetr)	1.14	86	2.17	1.978
VT-0.9	60	40, V^{5+} (tetr)	1.56	85	4.07	1.977
VT-1.9	19	81, V^{5+} (tetr)	2.60	86	9.06	1.960
VT-4.2	25	65, V^{5+} (oct) 10, V$_2$O$_5$	2.45	88	4.53	1.955
VT-6.1	0	47, V^{5+} (oct) 53, V$_2$O$_5$	2.38	87	5.07	1.955
VT-12.4	0	26, V^{5+} (oct) 74, V$_2$O$_5$	1.91	88	18.12	1.955
VTM	0	100, V^{4+} (tetr)	4.05	79		

being present. The selectivity reaches a maximum for the vanadyl phase in samples Vt-4.2, 6.1, and 12.4. Also, there seems to be a correlation between total spin concentration and the reaction rate within the tetrahedral phase; that is both increase up to a coverage of 1.5 layers. Within the octahedral phase, a similar correlation is evident. The samples labelled VT-4.2 and VT-6.1 have similar spin concentrations and similar rates.

Comparison of the surface concentration of reduced vanadium with the total magnetic susceptibility suggest that at low coverage, aggregation or island formation is probable. While the magnetic susceptibility increases, the amount of V^{4+} in the surface decreases, suggesting the clustering of vanadia species. This result is supported by chemical analyses which show the total V^{4+} to increase with vanadia loading. Comparison of low coverage, <1.5 layers to the true monolayer sample reinforce this conclusion. Here, chemical analysis suggests the surface is entirely reduced vanadia in a tetrahedral coordination. The EPR spectral data support this.

EPR studies on the catalysts following their use in ammoxidation, show two reso-

nances up to coverages of five monolayers. The sharp feature which is readily apparent in the five-layer catalyst, and distinguishable down to 0.5 layers, is absent or muted in the fresh catalysts. Whether this observation is suggesting increased reactivity for a specific coordination state of vanadium affecting one state primarily, or is correlated with a structural reconstruction of vanadia states is yet to be determined, but it is clear from these measurements, that significant chemical change occurs at the V^{4+} sites under ammoxidation conditions.

Further, analysis of the monolayer suggested that the mode of preparation seriously affects the magnetic character of the vanadium states. For all coverages below 3.5 theoretical layers, sharp hyperfine features were observed indicated localization or isolation of V^{4+} states. In the monolayer produced from the ammonia washing of a five-layer sample, the hyperfine structure is not clearly resolved. The spectrum of the true monolayer seems to be dominated by a broad resonance.

Fierro et al. (20) have studied monolayer states of vanadia supported on silica prepared by impregnation methods. In this work, the EPR parameters were strongly

affected by sample treatment with the general observation, being that isolated V^{4+} species can be observed in all freshly prepared samples. Busca et al.(22) have shown that for V_2O_5 supported on TiO_2(rutile), the first monolayer is dominated by VO^{2+} species. Ammonia washing for 5, 15, and 25% V_2O_5 samples showed the presence of insoluble V^{4+} species, usually indicative of aggregate or cluster formation. For the lowest concentration, the washed sample showed a simpler EPR spectrum with resolved hyperfine components, arising from a single type of vanadium species which is magnetically isolated.

In this study, the true monolayer of vanadia on TiO_2(B) shows the effects of dipolar exchange. This suggests the character of the monolayer is strongly dependent on the method of preparation. The FTIR studies have shown that at high loadings the V_2O_5 structure is observed, with octahedral and tetrahedral states being maintained at the lower loadings, and the monolayer produced by ammonia washing should be a more regular layer in which V^{4+}–V^{4+} interactions dominate. The monolayer produced from impregnation demonstrates the effect the support has in the catalyst design. Below the 1.5-layer limit, the surface is not completely covered and thus isolated V^{4+} centers and a small percentage of species originating from the dipolar interactions of the vanadium centers are observed. For the monolayer produced by ammonia washing, a regular structure is expected and thus the limit of dipolar exchange increases providing the spectral features observed. These observations suggest that domain formation is occurring below the monolayer limit and may help to rationalize the presence of multiple species magnetic species in vanadia aggregates.

CONCLUSION

In this work, EPR results were presented on a series of vanadia/TiO_2(B) catalysts and a correlation of the EPR results with structural data was made. This is the first EPR study of V_2O_5 on TiO_2(B), and it has shown that use of the TiO_2(B) phase as a support produces a variety of V^{4+} and V^{5+} species as a function of coverage and preparation. Chemical analyses coupled with IR measurements have shown a maximum of V^{4+} states with tetrahedral coordination in the low coverage limit. At low coverages the V^{4+}/V^{5+} reached a maximum. At higher coverages, V^{5+} dominated and the formation of bulk V_2O_5 was observed. The EPR study showed spectral features and trends similar with those of the earlier catalytic and structural (IR) studies (9). Multiple magnetic species were observed. At low coverages two species were observed, one of which may be attributable to a tetrahedral coordination. At the higher coverage, the EPR suggested the formation of bulk V_2O_5. In these studies a maximum in V^{4+} was observed at 1.5 monolayers, and the decrease in spin concentration above that limit suggests the formation of a new vanadia phase or new magnetic species associated with a structural change. A correlation between the magnetic density and catalytic reactivity shows a strong relationship between spin concentration and activity and their remains a focus of continued study, as does further characterization of the coverage induced phases.

REFERENCES

1. Bond, G. C., and König, P., J. Catal. 77, 309 (1982).
2. Gasior, M., Gasior, I., and Grzybowska, B., Appl. Catal. 10, 87 (1984).
3. Saleh, R. Y., and Wachs, I. E., Appl. Catal. 31, 87 (1987).
4. Papachryssanthou, J., Bordes, E., Vejux, A., Courtine, P., Marchand, R., and Tournoux, M., Catal. Today 3, 219 (1987).
5. van Hengstum, A. J., van Ommen, J. G., Bosch, H., and Gellings, P. J., Appl. Catal. 8, 369 (1983).
6. Mori, K., Miyamoto, A., and Murakami, Y., J. Chem. Soc. Faraday Trans. 1 83, 3303 (1987).
7. Jonson, B., Rebenstorf, B., Larsson, R., and An-

dersson, S. L. T., *J. Chem. Soc. Faraday Trans. 1* **84**, 3547 (1988).

8. Cavani, F., Foresti, E., Trifiro, F., and Busca, G., *J. Catal.* **106**, 251 (1987).

9. Sanati, M., and Andersson, A., *J. Mol. Catal.* **59**, 233 (1990).

10. Cavani, F., Centi, G., Foresti, E., Trifiro, F., and Busca, G., *J. Chem. Soc. Faraday Trans. 1* **84**, 237 (1988).

11. Andersson, A., Bovin, J.-O., and Walter, P., *J. Catal.* **98**, 204 (1986).

12. Kozlowski, R., Pettifer, R. F., and Thomas, J. M., *J. Phys. Chem.* **87**, 5176 (1983).

13. Bond, G. C., Zurita, J. P., Flamerz, S., Gellins, P. J., Bosch, H., van Ommen, J., and Kip, B. J., *Appl. Catal.* **22**, 361 (1986).

14. Busca, G., Centi, G., Marchetti, L., and Trifiro, F., *Langmuir* **2**, 568 (1986).

15. Haber, J., Kozlowska, A., and Kozlowski, R., *J. Catal.* **102**, 52 (1986).

16. Wachs, I. E., Saleh, R. Y., Chan, S. S., and Chersich, C. C., *Appl. Catal.* **15**, 339 (1985).

17. Schraml, M., Fluhr, W., Wokaun, A., and Baiker, A., *Ber. Bunsenges. Phys. Chem.* **93**, 852 (1989).

18. Matsuda, S., and Kato, A., *Appl. Catal.* **8**, 149 (1983).

19. Gasior, M., Haber, J., and Machej, T., *Appl. Catal.* **33**, 1 (1987).

20. Fierro, J. L. G., Gambaro, L. A., Gonzalez-Elipe, A. R., and Soria, J., *Colloids Surf.* **11**, 31 (1984).

21. Rusiecka, M., Grzybowska, B., and Gasior, M., *Appl. Catal.* **10**, 101 (1984).

22. Busca, G., and Marchetti, L., and Centi, G., Trifiro, F., *J. Chem. Soc. Faraday Trans. 1* **81**, 1003 (1985).

23. Chary, K. V. R., Mahipal Reddy, B., Nag, N. K., Subrahmanyam, V. S., and Sunandana, C. S., *J. Phys. Chem.* **88**, 2622 (1984).

24. Hisashi, U., *Bull. Chem. Soc. Jpn.* **52**, 1905 (1979).

25. Serwicka, E., and Schindler, R. N., *Z. Naturforsch. A* **36**, 992 (1981).

26. Dryek, K., Serwicka, E., and Grzybowska, B., *React. Kinet. Catal. Lett.* **10**, 93 (1979).

27. Sharma, V. K., Wokaun, A., and Baiker, A., *J. Phys. Chem.* **90**, 2715 (1986).

28. Narayana, M., Narasimhan, C. S., and Kevan, L., *J. Chem. Soc. Faraday Trans 1* **81**, 137 (1985).

29. Tronconi, E., Elmi, A. S., Natale, F., and Forzatti, P., Busca, G., Tittarelli, P., *Ind. Eng. Chem. Res.* **26**, 1269 (1987).

30. Iwamoto, M., Takenaka, T., Matsukami, K., Hirata, J., Kagawa, S., and Izumi, J., *Appl. Catal.* **16**, 153 (1985).

31. Piechotta, von M., Ebert, I., and Scheve, J., *Z. Anorg. Allg. Chem.* **368**, 10 (1969).

32. Yabrov, A. A., Ismailov, E. G., Boreskov, G. K., Ivanov, A. A., and Anufrienko, V. F., *React. Kinet. Catal. Lett.* **3**, 237 (1975).

33. Bond, G. C., and Sarkany, A. J., *J. Catal.* **57**, 476 (1979).

34. Marchand, R., Brohan, L., and Tournoux, M., *Mater. Res. Bull.* **15**, 1129 (1980).

35. Powder Diffraction File, No. 32-861, JCPDS International Centre for Diffraction Data, Swarthmore, 1985.

36. Powder Diffracton File, No. 35-88, JCPDS International Centre for Diffraction Data, Swarthmore, 1985.

37. Program supplied by N. D. Cheyney.

38. Neiman, R., Kivelson, D., *J. Chem. Phys.* **35**, 149, 156, 162 (1961).

39. Bleaney, B., *Philos. Mag.* **42**, 441 (1951).

40. Rollman, L. D., and Chan, S. I., *J. Chem. Phys.* **50**, 3416 (1969).

41. Mahootian, N., Kikuchi, C., Viehmann, W., *J. Chem. Phys.* **48**, 1097 (1968).

42. Holloway, C. E., Mabbs, F. E., Smail, W. R., *J. Chem. Soc. (A)*, 2980 (1968).

43. Petersen, J. L., Dahl, L. F., *J. Am. Chem. Soc.* **97**, 6422

44. Shuddhodan, M., Shri, N. S., Evans, J. C., Rowlands, C., *J. Mol. Struct.* **112**, 59 (1984).

45. Evans, A. G., Evans, J. C., Espley, D. J. C., Morgan, P. H., Mortimer, J., *J. Chem. Soc. Dalton. Trans.*, 57 (1978).